Chin. Geogra. Sci. 2011 21(6) 753–764
doi: 10.1007/s11769-011-0509-6
www.springerlink.com/content/1002-0063

Spatial-temporal Characteristics of Land Subsidence Corresponding to Dynamic Groundwater Funnel in Beijing Municipality, China

CHEN Beibei[1, 2, 3], GONG Huili[1, 2, 3], LI Xiaojuan[1, 2, 3], LEI Kunchao[1, 2, 3], ZHANG Youquan[1, 2, 3], LI Jiwei[1, 2, 3], GU Zhaoqin[1, 2, 3], DANG Yanan[1, 2, 3]

(*1. Base of the State Key Laboratory of Urban Environmental Process and Digital Modeling, Capital Normal University, Beijing 100048, China; 2. Key Laboratory of 3D Information Acquisition and Application, Ministry of Education, Capital Normal University, Beijing 100048, China; 3. College of Resource Environment and Tourism, Capital Normal University, Beijing 100048, China*)

Abstract: Due to long-term over-exploitation of groundwater in Beijing Municipality, regional groundwater funnels have formed and land subsidence has been induced. By combining a groundwater monitoring network, GPS monitoring network data, radar satellite SAR data, GIS and other new technologies, a coupled process model based on the dynamic variation of groundwater and the deformation response of land subsidence has been established. The dynamic variation of groundwater funnels and the land subsidence response process were analyzed systematically in Beijing. Study results indicate that current groundwater funnel areas are distributed mainly in the southwest of Shunyi District, the northeast of Chaoyang District and the northwest of Tongzhou District, with an average decline rate of groundwater level of 2.66 m/yr and a maximum of 3.82 m/yr in the center of the funnels. Seasonal and interannual differences exist in the response model of land subsidence to groundwater funnels with uneven spatial and temporal distribution, where the maximum land subsidence rate was about –41.08 mm/yr and the area with a subsidence rate greater than 30 mm/yr was about 1637.29 km^2. Although a consistency was revealed to exist between a groundwater funnel and the spatial distribution characteristics of the corresponding land subsidence funnel, this consistency was not perfect. The results showed that the response model of land subsidence to the dynamic variation of groundwater was more revealing when combining conventional technologies with InSAR, GIS, GPS, providing a new strategy for environmental and hydrogeological research and a scientific basis for regional land subsidence control.

Keywords: land subsidence; groundwater funnel; over-exploitation of groundwater; InSAR; deformation response

Citation: Chen Beibei, Gong Huili, Li Xiaojuan, Lei Kunchao, Zhang Youquan, Li Jiwei, Gu Zhaoqin, Dang Yanan, 2011. Spatial-temporal characteristics of land subsidence corresponding to dynamic groundwater funnel in Beijing Municipality, China. *Chinese Geographical Science*, 21(6): 753–764. doi: 10.1007/s11769-011-0509-6

1 Introduction

Land subsidence is a non-compensable and permanent change that can affect both local environment and resources. The process could even constitute a regional environmental disaster caused by a failure of the geological system, and such environmental disasters can occur in a series, thereby inducing a disaster chain. The results of many studies indicated that the over-exploitation of groundwater is the main reason for regional land subsidence (Chen, 2000; Xue, 2003). Gelt (1992) believed that long-term and large-scale over-exploitation of groundwater was the main cause of land subsidence, resulting in a significant decline of groundwater level,

Received date: 2011-03-30; accepted date: 2011-09-15
Foundation item: Under the auspices of Program of International S&T Cooperation (No. 2010DFA92400), Non-profit Industry Financial Program of the Ministry of Water Resources (No. 200901091), Beijing Municipal Natural Science Foundation (No. 8101002), Beijing Municipal Education Commission Plans to Focus Science and Technology Projects (No. KZ201010028030), National Natural Science Foundation of China (No. 41130744, 41171335)
Corresponding author: GONG Huili. E-mail: Gonghl@263.net

pore water saturation of the aquitard and aquifer and stress transfer leading to the deformation (compaction) of clay. At present, some new progress has been made in numerical modeling and monitoring technologies of land subsidence. The mathematical models of land subsidence include two parts: water flow modeling and soil mechanics modeling. Through research on the relationship between groundwater over-exploitation and the deformation of an aquitard and aquifer system caused by aquifer level variations, laws and development trend of land subsidence have been studied and predicted. Based on land subsidence monitoring networks established on bedrock, stratified and grounded benchmarks, various land subsidence monitoring methods have been combined with the development of Global Positioning System (GPS) and interferometric synthetic aperture radar (InSAR) technologies, providing new technical methods for investigation and monitoring of land subsidence.

The lack of observational data has made it difficult in the past to accurately define the extent of deformation, the magnitude of surface displacements, and seasonal land-surface motions with high spatial and temporal resolution. Persistent scatterer (PS) interferometry, which is an extension of the conventional differential synthetic aperture radar interferometry (D-InSAR) technique, can reduce the spatial and temporal decorrelation and weaken the error that occurs as the result of atmospheric delay, while enhancing spatial and temporal resolution. A large number of studies showed that with the development of new synthetic aperture radar (SAR) sensors and interferometric SAR techniques, the application of satellite radar data can now detect and monitor ground displacements at greater spatial detail (with centimeter to millimeter precision) and higher temporal resolution.

Many scholars at home and abroad have now used InSAR technology to monitor ground deformation (Hoffmann *et al*., 2001; Hopper *et al*., 2004). Ferretti *et al*. (2001) presented the concept of persistent scatterer interferometry, which can reduce spatial and temporal decorrelation, weaken the error that occurs as a result of atmospheric delay, and enhance temporal and spatial resolution. Hooper *et al*. (2004) proposed a new method to identify PS pixels and analysis phase composition—StamPS, which establishes a PS recognition algorithm by amplitude dispersion characteristics and spatially correlated features of interferometry phase. The method resolves the problem in interferometry caused by temporal decoherence, which can increase the available quantity of image pixels and improve the temporal resolution of the interference.

During the last two decades, many foreign scholars have undertaken the researches that involve both InSAR and hydrogeology. In particular, they have studied the causes and evolutionary characteristics of regional land subsidence events. Many studies have demonstrated that InSAR technology can measure surface displacements deformation related to an aquifer-system accompanying groundwater discharge and recharge (Galloway *et al*., 2000; Watson *et al*., 2002; Schmidt and Bürgmann, 2003; Chang and Chang, 2004). Other studies have revealed the water release deformation mechanism of groundwater aquifer systems (Stramondo, 2008; Yan and Burbey, 2008), and qualitatively and quantitatively analyzed the changes in a groundwater aquifer systems and the corresponding response mechanisms of land subsidence.

Currently, land subsidence has been documented in 95 cities in China. In order to understand land subsidence in different regions of China, a series of studies making use of regional land subsidence monitoring technology and subsidence modeling has been conducted with outstanding practical achievements (Li *et al*., 2004; Gong *et al*., 2009), and a more complete monitoring, analysis, and forecasting system has been formed. For example, Beijing is a metropolis with a serious water shortage, where the urban per-capita water resources is 248 m^3, equivalent to only 1/8 of the national level and 1/16 of the global level. Two-thirds of the water supply comes from groundwater in Beijing. Therefore the exploitation of groundwater leading to water level decline is a key factor in the formation and development of land subsidence (Jia *et al*., 2007).

In this paper, by combining groundwater monitoring network, GPS monitoring network data, radar satellite SAR data and GIS, the coupling process model based on dynamic variation of groundwater and deformation response of land subsidence were established in this study, where dynamic variation of groundwater funnel in Beijing were analyzed systematically as well as land subsidence response process. The research results are more beneficial to reveal the response model of land subsi-

dence to dynamic variation of groundwater by combining conventional technologies with InSAR, GIS, GPS and other new technologies, providing a new technology for environmental and hydrogeological research and a scientific basis for regional land subsidence control.

2 Materials and Methods

2.1 Study area

2.1.1 Geographic and meteorological setting

Beijing (39°28'–41°05'N, 115°25'–117°35'E) is located in the northern part of the North China Plain, which is divided into the western mountains, northern mountains and plains of the southeast (Fig. 1). The seasonal distribution of precipitation is uneven in the study area. Concentrated precipitation from June to August generally accounts for 70% of the annual total. From 1999 to 2006, eight consecutive years of drought conditions occurred in Beijing. The eight-year average precipitation in Beijing was 459.11 mm, equivalent to 84.2% of the long-term average.

2.1.2 Hydrogeological background

Groundwater in Beijing is found in an upper unconfined aquifer and lower confined aquifers. The aquifer system of the upper layer includes alluvial fan sediments dominated by sandy gravels, with a water table of 5–20 m. A middle aquifer layer consist of a sandy-gravel/sand formation capped by a clayey stratum. Within the approximately 100-m-thick unit, the thickness of aquifer is 40 m, and the depth of the top of groundwater is 5–15 m below the top of the unit; permeability and water abundance in the aquifer is good. Other formations of 2- to 3-m-thick sands capped by clayey strata are numerous; however, permeability and water abundance of these aquifer layers is poor (Xie *et al*., 2003).

2.2 Methods

2.2.1 Mathematical modeling

(1) Groundwater numerical model. As over-exploitation of groundwater is serious in the study area, data from the groundwater monitoring network can not accurately describe the groundwater flow field. Instead, a numerical model is needed to simulate the development of groundwater funnels. Groundwater flow in the study area was assumed to be a three-dimensional (3D) unsteady stream process. Modular three-dimensional groundwater flow model (MODFLOW) (Equation (1)), developed by the United States Geological Survey (USGS) (Michael G *et al*., 1988) was used to simulate the seepage field of regional aquifer systems. It has been used to simulate and analyze the evolution of groundwater from 2003 to 2006 in the study area.

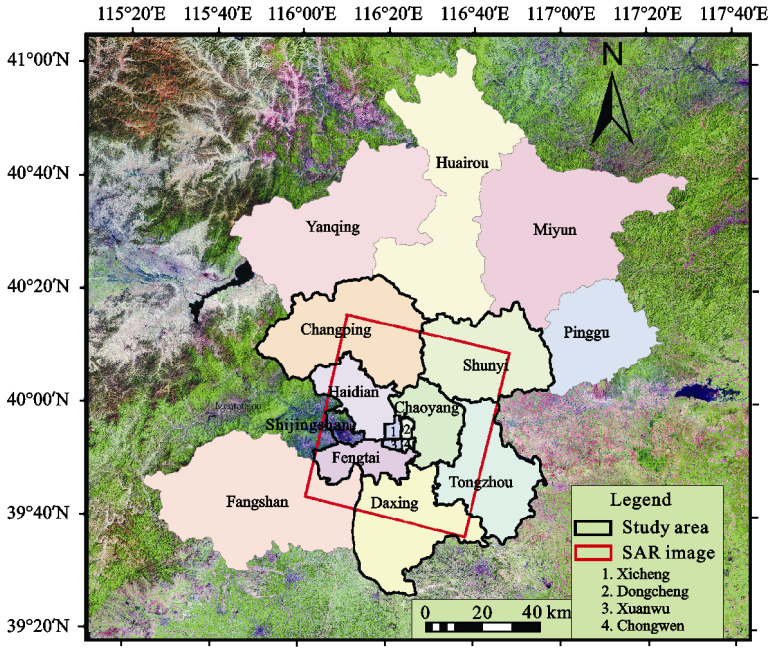

Fig. 1 Location of study area in Beijing

$$\begin{cases} S\dfrac{\partial h}{\partial t}=\dfrac{\partial}{\partial x}\left(K_x\dfrac{\partial h}{\partial x}\right)+\dfrac{\partial}{\partial y}\left(K_y\dfrac{\partial h}{\partial y}\right)+ \\ \qquad \dfrac{\partial}{\partial z}\left(K_z\dfrac{\partial h}{\partial z}\right)+\varepsilon & x,y,z\in\Omega,t\ge 0 \\ \mu\dfrac{\partial h}{\partial t}=K_x\left(\dfrac{\partial h}{\partial x}\right)^2+K_y\left(\dfrac{\partial h}{\partial y}\right)^2+ \\ \qquad K_z\left(\dfrac{\partial h}{\partial z}\right)^2-\dfrac{\partial h}{\partial z}(K_z+p)+p & x,y,z\in\Gamma_0,t\ge 0 \\ h(x,y,z,t)\big|_{t=0}=h_0 & x,y,z\in\Omega,t\ge 0 \\ K_n\dfrac{\partial h}{\partial \vec{n}}\Big|_{\Gamma_1}=q(x,y,z,t) & x,y,z\in\Gamma_1,t\ge 0 \\ \dfrac{\partial h}{\partial \vec{n}}\Big|_{\Gamma_2}=0 & x,y,z\in\Gamma_2,t\ge 0 \end{cases} \quad (1)$$

where Ω indicates the seepage area (m^2); h indicates the water level elevation in the aquifer (m); K_x, K_y and K_z indicate the permeability coefficients in the x, y and z direction respectively (m/d); K_n indicates the permeability coefficient of the boundary surface in the normal direction (m/d); S indicates the specific storage of aquifer under free surface (L/m), when the water level is higher than the previous minimum level, S is the elastic storage, whereas when the water level is lower than the previous minimum level, S is the non-elastic storage; μ indicates the specific yield of the phreatic aquifer over the water table; ε indicates the source sink term of the aquifer (L/d); p indicates the evaporation and rainfallof the water table (L/d); h_0 indicates the initial distribution of aquifer water level (m); Γ_0 indicates the upper boundary of the seepage area, i.e., the free surface of groundwater; Γ_1 indicates the mixed boundary of the water-bearing body; Γ_2 indicates the lower boundary of the seepage area, i.e., the impervious boundary at the bottom of confined aquifer; $\vec{n}$ indicates the normal direction of the boundary surface.

(2) The InSAR deformation monitoring model for land subsidence. Due to the over-exploitation of groundwater in the water system of the study area, the local aquitard was consolidated, leading to aquifer compression and land subsidence. Persistent Scatterers for SAR Interferometry (PSInSAR) can effectively reduce the spatial and temporal decorrelation effects and weaken the error component caused by atmospheric delay. By applying error corrections to the atmospheric, orbital and digital elevation model (DEM), determinations of accurate deformation (including its rate) can be extracted relative to specific ground reference points, so as to obtain the deformation phase component (Equation (2)) (Hooper *et al*., 2004). Stamps Method was used in this study, and the InSAR deformation monitoring model of land subsidence was established as follows (Fig. 2):

$$\phi_{x,i}=\phi_{\mathrm{def},x,i}+\phi_{\varepsilon,x,i}+\phi_{\mathrm{atm},x,i}+\phi_{\mathrm{orb},x,i}+\phi_{\mathrm{n},x,i} \quad (2)$$

where ϕ_{def} indicates the deformation phase in the viewing direction; ϕ_{ε} indicates the residual topographic phase caused by errors brought about by the introduction of an external DEM; ϕ_{atm} indicates the phase difference in atmospheric delays between two satellite transits; ϕ_{orb} indicates the phase caused by orbit error; and ϕ_{n} indicates the noise component.

In order to limit the effect of spatial and temporal decorrelation of the InSAR signal, suitable data pairs within the European Space Agency (ESA) archives have been selected by a cross check of perpendicular baselines vs. time intervals. A total of 14 ENVISAT-Advanced Synthetic Aperture Radar (ENVISAT-ASAR) raw data sets covering the study area from descending satellite track 2218 and frame 2799 were received from ESA. The interferometric phase is formed by 16 images with a normal baseline ranging from –450 m to 333 m with respect to the master acquisition acquired on 2005-12-14. Precise satellite orbits were provided by the University of Delft. The topographic phase contribution was removed using the 3 s (90 m) Shuttle Radar Topography Mission (SRTM) DEM.

2.2.2 Comprehensive analysis model

A combination of routine long-term dynamic monitoring, simulations, prediction technologies of groundwater system, InSAR, GIS and other new technologies enabled the construction of the spatial data field. Based on the coupled model between dynamic variations of groundwater and the deformation response of land subsidence, a systematic analysis of dynamic variations in the Beijing groundwater funnel and the evolutionary process of land subsidence response in the study area have been undertaken (Fig. 3).

3 Results and Analyses

3.1 Formation and dynamic variation of groundwater funnel

Based on a long time-series of monitoring data, GIS and

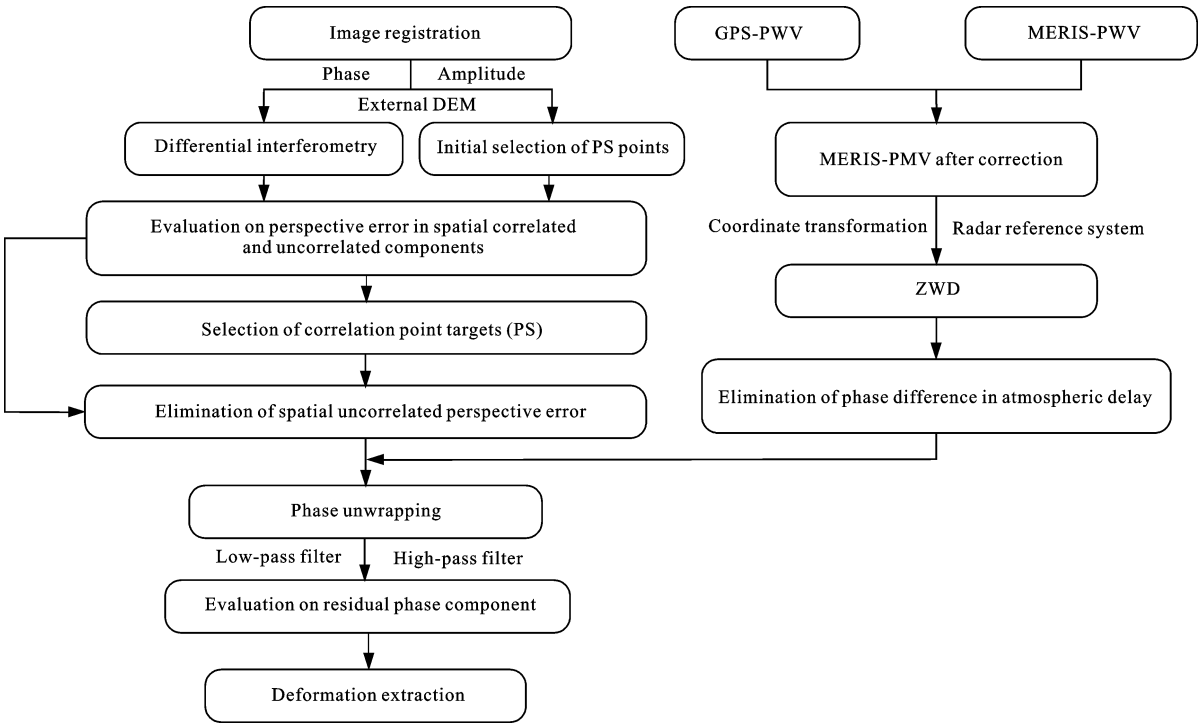

PWV: Precipitable water vapor; MERIS: Medium resoulution imaging spectrometer;
ZWD: Zenith wet delay; PS: Persistent scatterers

Fig. 2 InSAR deformation monitoring model of land subsidence

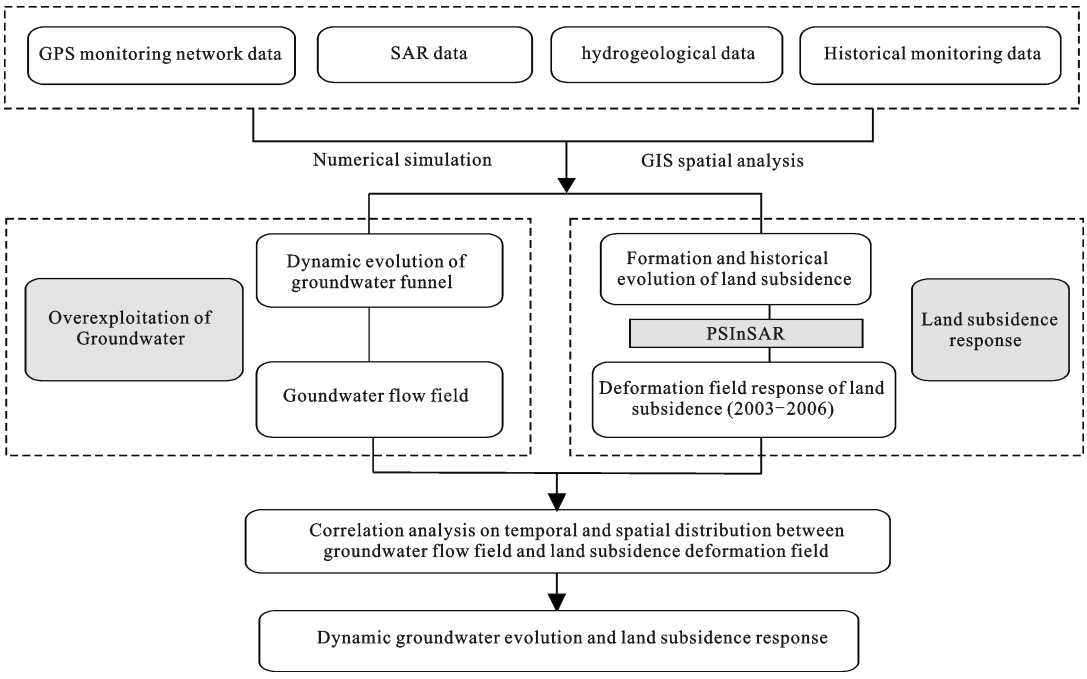

SAR: Synthetic aperture radar; GIS: Geographic Information System;
PSINSAR: Persistent scatterers for SAR Interferometry

Fig. 3 Framework diagram of comprehensive analysis model

groundwater numerical simulation technologies were used to investigate the formation and dynamic variation of groundwater funnel in Beijing.

As shown in Fig. 4, a significant groundwater funnel had formed in the study area in 1975, with a buried water-level depth of 23.75 m at the center of the funnel and an area of about 250 km^2. By 2001, the water-level depth at the center of the groundwater funnel had increased to 43.60 m, and the area had expanded to about 1000 km^2. It could be assumed that, due to overexploitation, groundwater funnels evolved rapidly since their local formation prior to 1975 until the early 21st century. Water levels have continued to decline (i.e., the buried water-level depth has continued to increase) and affected areas have continued to expand.

The spatial-temporal evolutionary features of groundwater depression in Beijing (Fig. 5) were revealed by GIS-based spatial analysis. As shown in Fig. 5, a large groundwater funnel was formed in Balizhuang, Chaoyang District by 1975 with an area of 250 km^2. The spatial distribution of the funnels was mainly developed towards the eastern suburbs with a propagation rate of 12.5 km^2/yr until 1985. Over the next decade, the groundwater funnel radially extended eastward and northward with an approximate propagation rate of 34 km^2/yr. In 2001, with the rapid increase of groundwater exploitation in suburbs, the funnel was distributed all over Shunyi District, western Changping District, Tongzhou District and eastern Chaoyang District, covering an area of 1000 km^2.

3.2 Evolution of land subsidence funnel

The land subsidence funnels in Dongbalizhuang-Dajiaoting of Chaoyang District and in Laiguangying of Shunyi District are the most representative funnels in Beijing, which have the longest subsidence history. However, even though new subsidence areas in the suburbs of Beijing (Shahe-Baxianzhuang of Changping District, Yufa-Lixiandi of Daxing District, Pinggezhuang of Shunyi District) formed later, they did develop very rapidly. GIS-based spatial analyses and routine monitoring data revealed the formation as well as the spatial and temporal evolutionary features of the above five land subsidence funnels (Fig. 6 and Fig. 7).

As shown in Fig. 6, the land subsidence funnel in Dongbalizhuang-Dajiaoting of Chaoyang District was locally formed in 1955–1966 with a settlement of 58 mm and the local subsidence rate of 4.8 mm/yr. After the mid-1980s, accompanied by an increase of groundwater exploitation in suburbs, groundwater exploitation was out of control in those areas (Beijing Bureau of Geology and Mineral Exploration and Development, Hydrogeology and Engineering Geology Team in Beijing, 2008). Thus, the cumulative settlement of land subsidence was increased year by year, but the subsidence rate declined. With the arrival of dry year in 1999, the groundwater level continued to decline with deteriorated land subsidence again. In six years (1999 to 2005), the settlement was 392 mm, the subsidence rate was increased to 56.3 mm/yr, and the maximum cumulative settlement reached 750 mm.

The formation and evolutionary process of the land subsidence funnel in Laiguangying were similar to those of Dongbalizhuang. It was formed from 1967 to 1973 with a subsidence rate of 16 mm/yr and a settlement of 66 mm. Similarly, after the mid-1980s, groundwater exploitation was controlled in this area, with a slowing trend of subsidence development. A continuous drought occurred in Beijing with little precipitation after 1998, and thus the development of the subsidence funnel was intensified again. In 2005, the land subsidence rate was up to about 65.4 mm in this area with the maximum cumulative settlement of 677 mm.

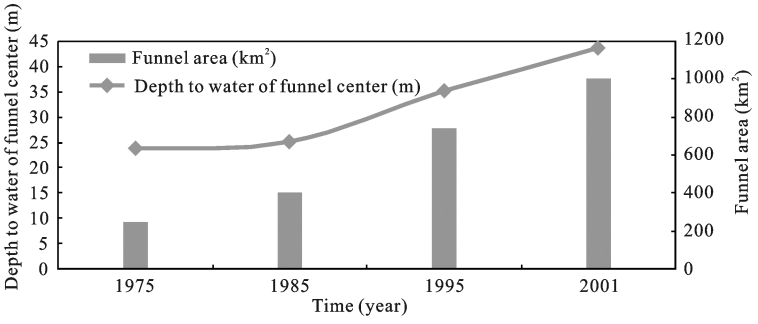

Fig. 4 Formation and evolution of groundwater funnel in Beijing

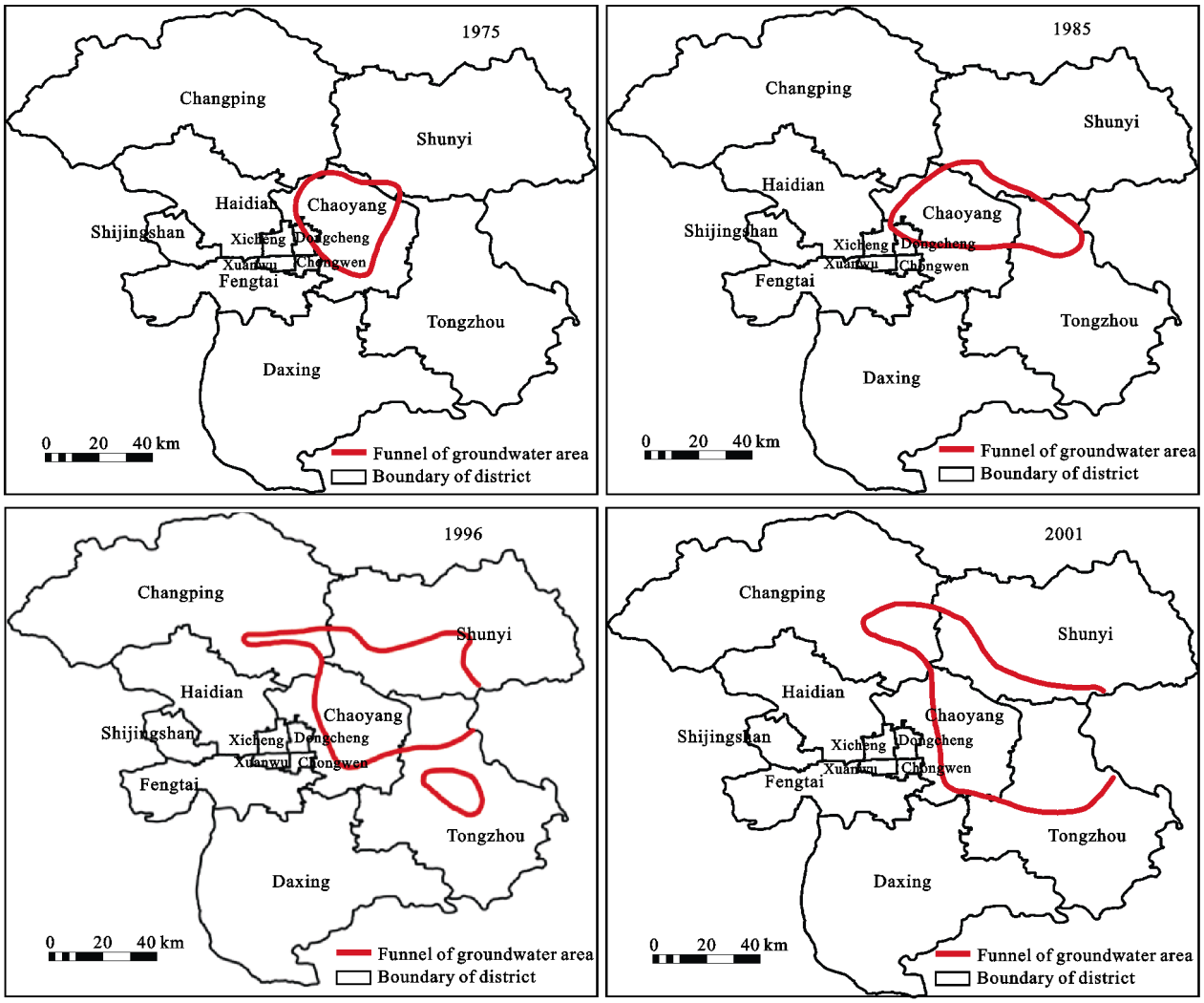

Fig. 5 Development and variation of groundwater funnels in Beijing in 1975–2001

From the late 1980s to the end of the 1990s, more stringent control measures were taken on groundwater exploitation in the eastern suburbs (Wang, 2004). With the reduction of exploitation, the water level decline rate slowed down as well as the land subsidence rate. However, in the meantime, some groundwater exploitation continued to increase in Beijing suburb areas during this period (such as Shahe of Changping District, and Yufa Town of Daxing District), so as to form several new subsidence areas with the representatives of Shahe-Baxianzhuang, Yufa-Lixian and Pinggezhuang, where subsidence had maintained rapid development. As shown in Fig. 7, by the end of 2005, the land subsidence funnels in Shahe-Baxianzhuang, Yufa-Lixian and Pinggezhuang had a subsidence rate of 66.3 mm/yr, 37 mm/yr and 28 mm/yr respectively. Among them, Shahe-Baxianzhuang had the maximum cumulative settlement of 1086 mm in Beijing with rapid subsidence development.

3.3 Acquisition of typical time-series spatial information for land subsidence

Integrating the development of the subsidence funnels found in the above five typical subsidence areas, the rapid development of subsidence in Beijing from 1999 to 2005 is readily seen. Combined with a transit baseline, archived data and other factors, a representative time series of the rapid development of Beijing land subsidence (2003–2006) was selected. Then, ASAR and SRTM data were used for interferometric processing in conjunction with the new Persistent Scatterers for SAR Interferometry (PSInSAR) technology (Hooper *et al.*, 2004). In this way, land subsidence deformation information was acquired for mutual validation and research

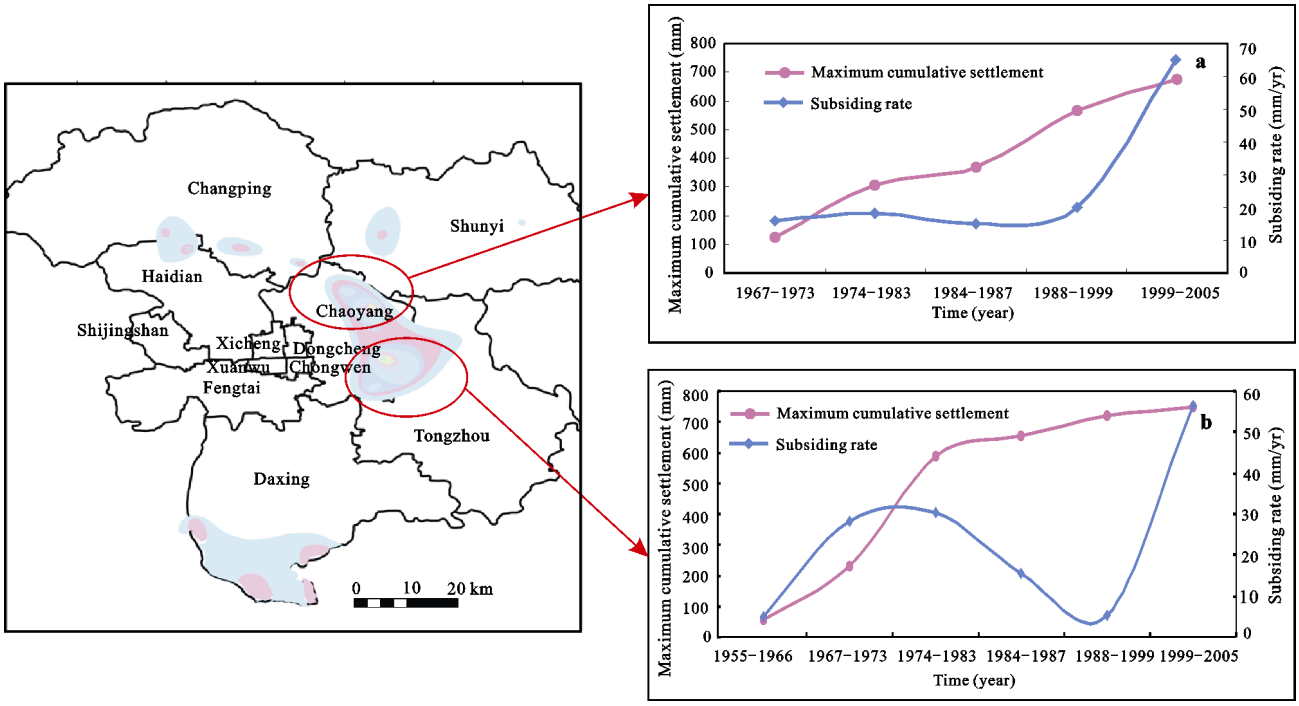

Fig. 6 Formation and evolution of land subsidence funnels in Dongbalizhuang-Dajiaoting (a) and Laiguangying (b)

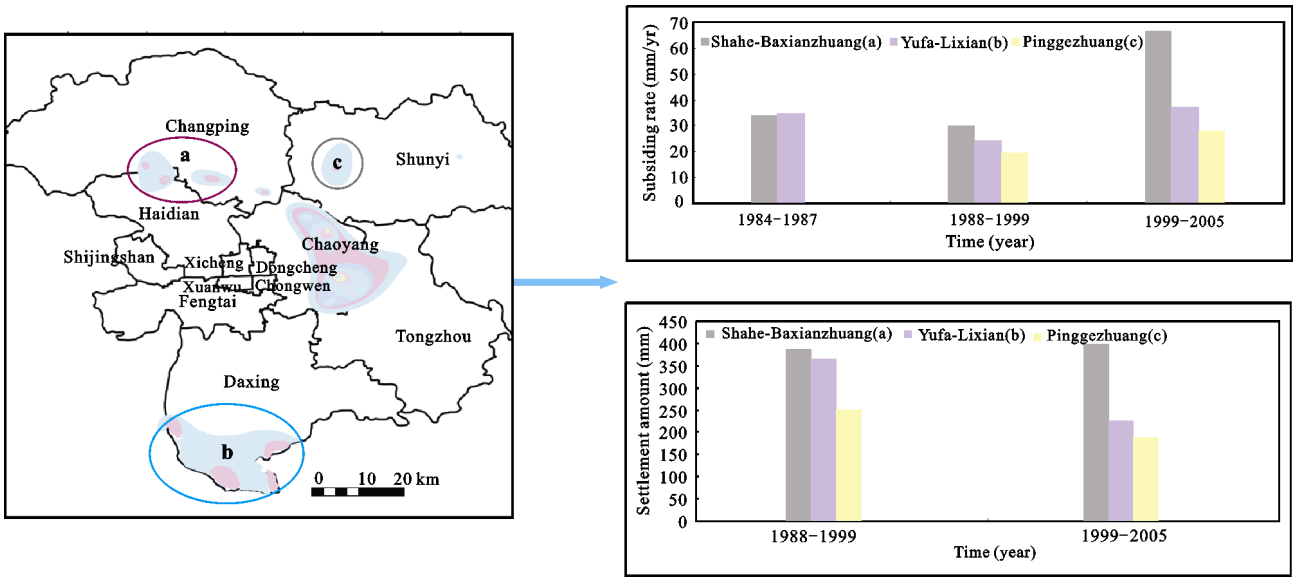

Fig. 7 Formation and evolution of land subsidence funnels

with historical routine subsidence in formation in order to reveal the spatial and temporal development trends of land subsidence in Beijing.

According to the analysis of InSAR time-series deformation results, land subsidence in Beijing shows such characteristics as seasonal fluctuations (as shown in the left side of Fig. 8), where the extent and amplitude of subsidence in autumn and winter were greater than those in spring and summer. For example, as shown in the purple box in the left side of Fig. 8, the amplitude and extent of the SAR image deformation on January 14, 2004 were significantly greater than those on July 7 of the same year. Meanwhile, the research results show a great difference in the rate of land subsidence in Beijing (as shown in the right side of Fig. 8) with a maximum subsidence rate of –41.08 mm/yr. The area of subsi-

dence with a rate greater than 30 mm/yr covered 1637.29 km^2, mainly distributed in Chaoyang, Shunyi, Changping and Tongzhou districts. In addition, InSAR time-series deformation results were relatively consistent with the trend of routine monitoring information leveling (shown as the purple contour in the right side of Fig. 8). InSAR, GIS technologies were used to further reveal the spatial evolutionary trend of land subsidence.

4 Discussion

Combining groundwater level contours for 2003–2006 with deformation results extracted by PS-InSAR for the same period, the correlation between land subsidence response trends and the groundwater flow field was analyzed comprehensively (Fig. 9). A serious and extensive subsidence in the land was revealed to have occurred in the areas with higher water depths, mainly in southwest of Shunyi District, northeast of Chaoyang District and northwest of Tongzhou District. It shows that variations of the groundwater flow field and the response process of land subsidence in Beijing is consistent.

After a triangulated irregular network (TIN) was created on groundwater level contours from 2003 to 2006, raster graphics operations were adopted to obtain dynamic variations of groundwater flow over the three-year period (Fig. 10). Moreover, the three-year trend of groundwater level decline was analyzed and combined with the trend in land subsidence to produce a comprehensive spatial analysis. The analysis showed that the spatial location of the groundwater funnels was not consistent with those of land subsidence funnels, with some noted variability (Fig. 10). Groundwater depression funnels were mainly located in southwest of Shunyi District, northeast of Chaoyang District and northwest of Tongzhou District. In recent years, the groundwater level has continued to decline in these areas with an average decline rate of 2.66 m/yr and a maximum of 3.82 m/yr at the center of the funnel. As is apparent from the InSAR time-series land subsidence trend (Fig. 9), land subsidence funnels not only occurred in the Shunyi and Chaoyang districts, but also in Tongzhou District where a very clear subsidence funnel had a maximum subsidence rate of –41.08 mm/yr. To a certain extent, groundwater exploitation in the Chaoyang subsidence funnel has been reduced in recent years, and the concentrated exploitation areas have been extended towards the northeastern suburbs. As a result, the extent of the Shunyi-Tongzhou subsidence funnel has expanded continuously.

Because a groundwater depression funnel can be affected by regional hydrogeological conditions, the thickness of compressible layers, stratum structure, the horizon of groundwater exploitation and other factors (Jiao and Qiu, 2006; Jia *et al*., 2007), it can closely re-

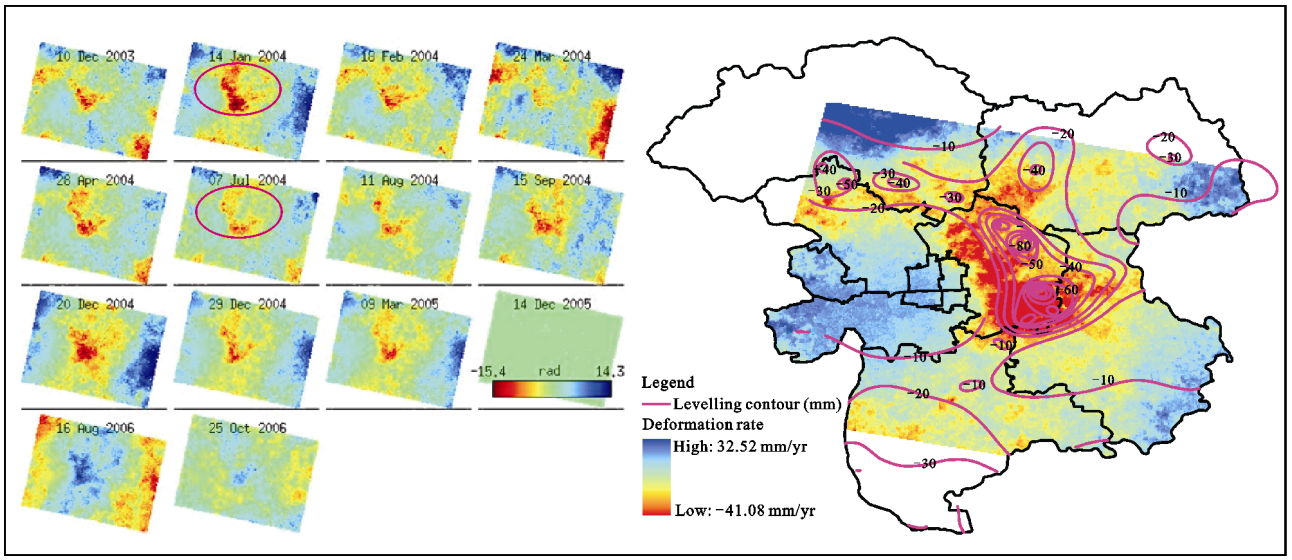

The left figure shows the deformation value and the right figure shows the deformation rate; the positive value in red indicates subsidence on the right side

Fig. 8 PS-InSAR land subsidence results for the study area

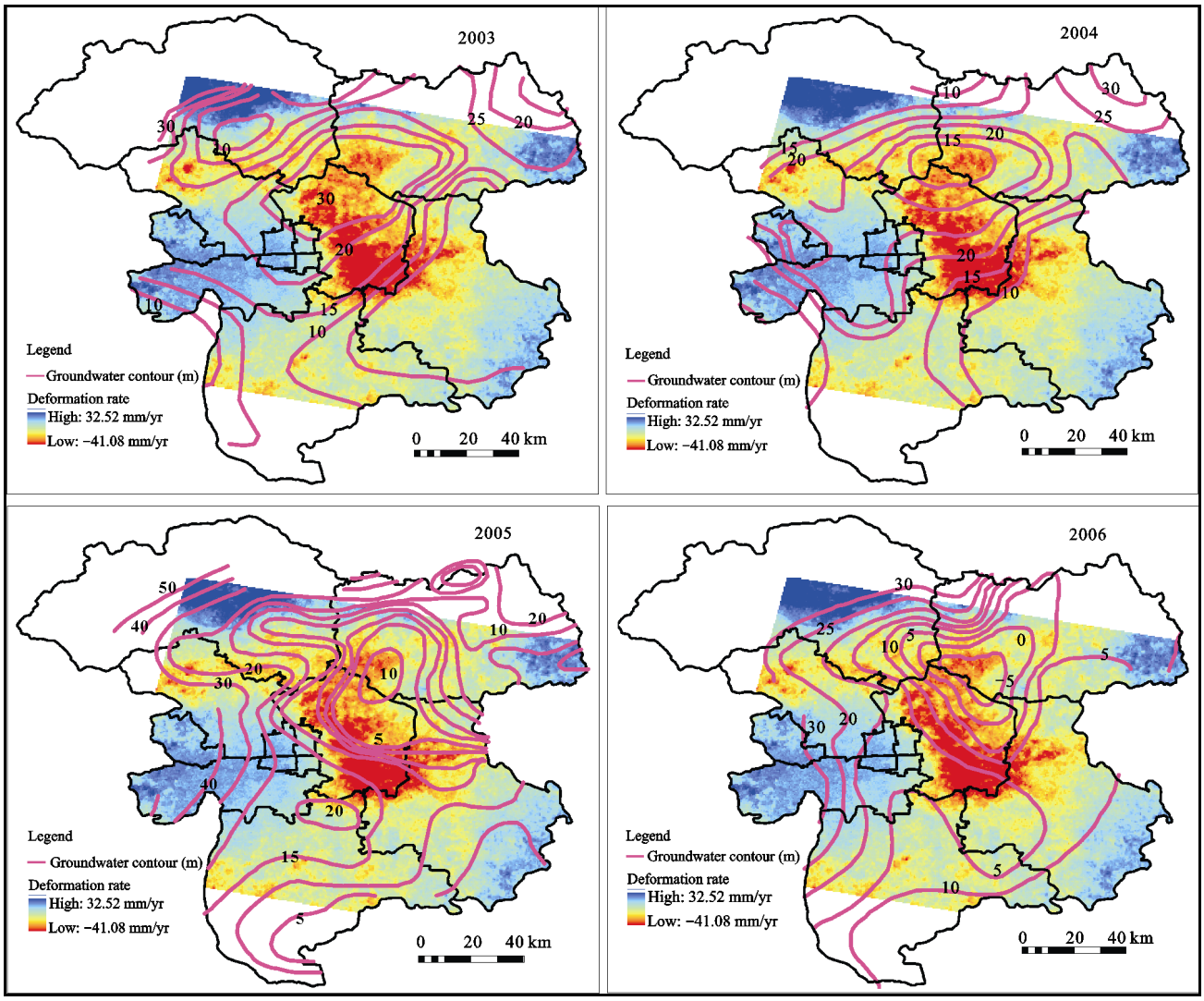

Fig. 9 Groundwater contours and land subsidence

flect the regional situation of land subsidence. However, the accurate description of the spatial distribution of settlement is difficult, as has been shown by attempts to invert settlement and groundwater level trends using InSAR technology (Fig. 10). Compared with the application of numerical simulation technology to land subsidence control (Gong *et al*., 2000; Shi *et al*., 2008), InSAR technology now plays a larger role in the acquisition of large-scale high-precision subsidence information. Therefore, InSAR data provide a good basis for land subsidence control and the monitoring of hazards. Combined with the spatial analysis capabilities of GIS technology (Oh and Lee, 2010), a better understanding of the spatial and temporal relationships between land subsidence and groundwater level were gained, thereby providing support for groundwater exploitation management decision.

5 Conclusions

By combining groundwater monitoring network, GPS monitoring network data, radar satellite SAR data, GIS and other new technologies, a coupled process model based on the dynamic variations of groundwater and deformation responses of land subsidence was established. This model is used to explain the spatial and temporal evolution of the groundwater depression funnel in Beijing as well as the 2D and 3D spatial response trends of land subsidence. The conclusions are drawn as follows:

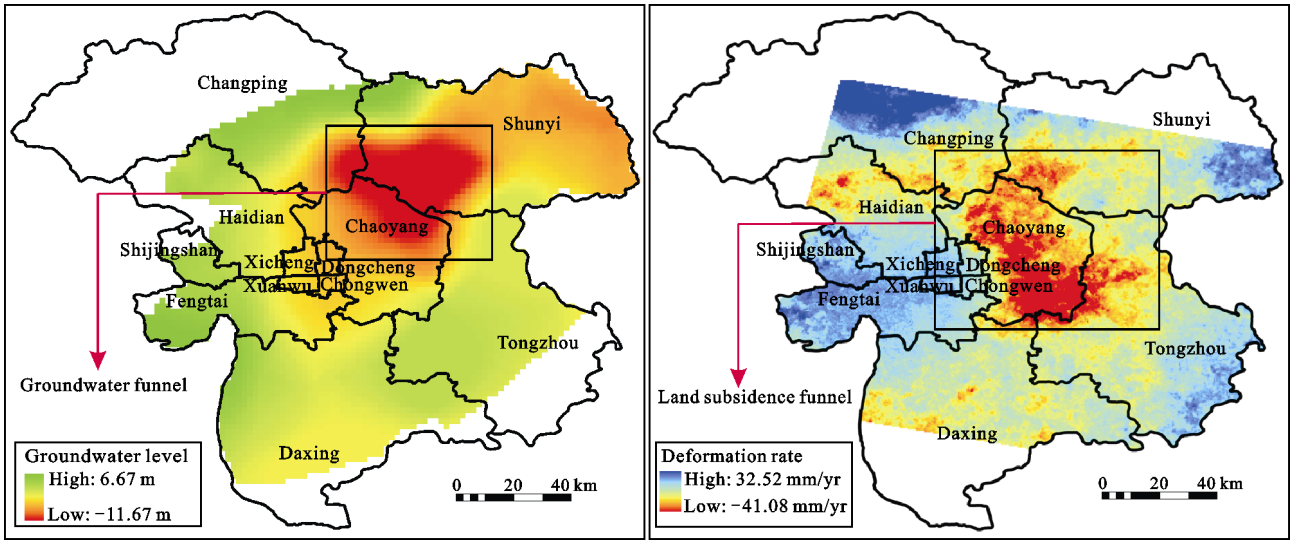

Fig. 10 Mean annual range of groundwater level and land subsidence in study area in 2003–2006

(1) The main groundwater funnel was formed prior to 1975 with an accelerating propagation rate (12.5–34.0 km^2/yr). The groundwater funnel covered an area of 1000 km^2 by 2001. From 2003 to 2006, the groundwater funnels were mainly distributed in southwest of Shunyi District, northeast of Chaoyang District and northwest of Tongzhou District, with the average decline rate of groundwater level of 2.66 m/yr and a maximum of 3.82 m/yr at the funnel center.

(2) The great seasonal and interannual differences exist in Beijing with uneven spatial and temporal distribution and a maximum subsidence rate of –41.08 mm/yr. The region of subsidence with a rate greater than 30 mm/yr covered 1637.29 km^2 and showed a trend of eastward movement.

(3) From a comparative analysis of the InSAR deformation response to land subsidence with the evolution of the interannual groundwater flow field, the groundwater funnel was revealed to be mostly consistent with the spatial distribution characteristics of the land subsidence funnel. Although the occurrence of land subsidence in Beijing is mainly due to the exploitation of groundwater, we proved that subsidence development could also correlate with hydrogeological conditions, stratal structures and so on. Additionally, a land subsidence response to the over-exploitation of groundwater may have a time delay. Further in-depth investigations of these issues are required in the future.

References

Beijing Bureau of Geology and Mineral Exploration and Development, Hydrogeology and Engineering Geology Team in Beijing, 2008. *Ground Water in Beijing*. Beijing: Land Press of China. (in Chinese)

Chang C P, Chang T Y, 2004. Land-surface deformation corresponding to seasonal ground-water fluctuation, determining by SAR interferometry in the SW Taiwan. *Mathematics and Computers in Simulation*, 67: 351–359.

Chen Chongxi, 2000. Thinking on land subsidence caused by groundwater exploitation. *Hydrogeology and Engineering Geology*, 27(1): 45–60. (in Chinese)

Ferretti A, Prati C, Rocca F, 2001. Permanent scatters in SAR interferometry. *IEEE Transactions on Geoscience and Remote Sensing*, 39(1): 8–20.

Galloway D L, Bürgmann R, Fielding E *et al*., 2000. Mapping recoverable aquifer-system deformation and land subsidence in Santa Clara Valley, California, USA, using space-borne synthetic aperture radar. *Proceedings of the 6th International Symposium on Land Subsidence, National Research Council of Italy* (*CNR*), 2: 229–236.

Gelt J, 1992. Land subsidence, earth fissures, change Arizona′s landscape. *Arroyo*, 6(2): 7–15.

Gong Huili, Li Menlou, Hu Xinli, 2000. Management of groundwater resources in Zhengzhou City, China. *Water Research*, 34(1): 57–62.

Gong Huili, Zhang Youquan, Li Xiaojuan *et al*., 2009. The research of land subsidence in Beijing based on permanent scatterers interferometric synthetic aperture radar (PS-InSAR) technique. *Progress in Natural Science*, 19(11): 1261–1266. (in Chinese)

Hoffmann Jorn , Zebker Howard A, Galloway Devin L *et al*., 2001. Seasonal subsidence and rebound in Las Vegas Valley, Nevada, observed by synthetic aperture radar interferometry. *Water Resources Research*, 37(6): 1551–1566.

Hooper A, Zebker H, Segall P *et al*., 2004. A new method for measuring information on volcanoes and other natural terrains using insar persistent scatterers. *Geophysical Research Letters*, 31: L23611. doi:10.1029/2004GL021737:

Jia Sanman, Wang Haigang, Zhao Shousheng *et al*., 2007. A tentative study of the mechanism of land subsidence in Beijing. *City Geology*, 2(1): 20–26. (in Chinese)

Jia Sanman,Wang Haigang, Luo Yong *et al*., 2007. The impacts of ground subsidence on urban construction in Beijing. *City Geology*, 2(4): 19–23. (in Chinese)

Jiao Qing, Qiu Zehua, 2006. Research progress of major active faults in Beijing Plain Area. *Institute of Crustal Dynamics*, CEA, 18: 72–84. (in Chinese)

Li Deren, Liao Mingsheng, Wang Yan, 2004. Progress of permanent scatterer interferometry. *Editorial Board of Geomatics and Information Science of Wuhan University*, 29(8): 664–668. (in Chinese)

Michael G McDonald, Arlen W Harbaugh, 1988. *A Modular Three-Dimensional Finite-Difference Ground-Water Flow Model*: *U.S. Geological Survey*, *Techniques of Water-Resources Investigations*. Scientific Publication.

Oh H, Lee S, 2010. Assessment of ground subsidence using GIS and the weights-of-evidence model. *Engineering Geology*, 115(1–2): 36–48. doi: 10.1016/j.enggeo.2010.06.015

Schmidt D A, Bürgmann R, 2003. Time dependent land uplift and subsidence in the Santa Clara Valley, California, from a large InSAR data set. *Journal of Geophysical Research*, 108(B9): 2416. doi: 10.1029/2002JB002267.

Shi X, Wu J, Ye S *et al*., 2008. Regional land subsidence simulation in Su-Xi-Chang area and Shanghai City, China. *Engineering Geology*, 100(1–2): 27–42. doi: 10.1016/j.enggeo.2008.02.011.

Stramondo S, 2008. Subsidence induced by urbanisation in the city of Rome detected by advanced InSAR technique and geotechnical investigations. *Remote Sensing of Environment*, 112(6): 3160–3172. doi: 10.1016/j.rse.2008.03.008.

Wang Ping, 2004. Study on land subsidence caused by overexploiting groundwater in Beijing. *Site Investigation Science and Technology*, (5): 46–49. (in Chinese)

Watson K M, Bock Y, Sandwell D T, 2002. Satellite interferometric observations of displacements associated with season groundwater in the Los Angeles Basin. *Journal of Geophysical Research*, 107(B4): 2074. doi: 10.1029/2001JB000470.

Xie Zhenhua, Ye Chao, Jia Sanman *et al*., 2003. Ground water resource and environmental investigation evaluation in Beijing. Beijing: Beijing Institute of Geological Survey. (in Chinese)

Xue Yuqun, Zhang Yun, Ye Shujun *et al*., 2003. Land subsidence in China and its problems. *Quaternary Sciences*, 23(6): 585–593. (in Chinese)

Yan Tingting, Thoma J Burbeys, 2008. The value of subsidence data in ground water model calibration. *Ground Water*, 46(4): 538–550. doi: 10.1111/j.1745-6584.2008.00439.x